

## Dual Fluorescence of 2-Methoxyanthracene Derivatives

Martin Albrecht,<sup>†</sup> Cornelia Bohne,<sup>\*,‡</sup> Anton Granzhan,<sup>§</sup> Heiko Ihmels,<sup>\*,§</sup> Tamara C. S. Pace,<sup>‡</sup> Alexander Schnurpfeil,<sup>†,||</sup> Michael Waidelich,<sup>§</sup> and Chang Yihwa<sup>‡</sup>

University of Siegen, Physical and Theoretical Chemistry, Adolf-Reichwein-Str., D-57068 Siegen, Germany, Department of Chemistry, University of Victoria, BC V8W 3V6, Canada, University of Siegen, Organic Chemistry II, Adolf-Reichwein-Str., D-57068 Siegen, Germany, and University of Cologne, Theoretical Chemistry, Greinstrasse 4, D-50939 Köln, Germany

Received: August 24, 2006; In Final Form: November 10, 2006

The time-resolved emission properties of selected anthracene derivatives, namely anthracene (**1a**), 2-methylanthracene (**1b**), 2-chloroanthracene (**1c**), 2-methoxyanthracene (**1d**), 2-methoxy-6-methylanthracene (**1e**), 2-(*N,N'*-dicyclohexylureidocarbonyl)-6-methoxyanthracene (**1f**), 2-(6-methoxyanthr-2-yl)-4,4-dimethyl-2-oxazoline (**1g**), 2-(6-methoxyanthr-2-yl)-pyridine (**1h**), and *N*-cyclohexylanthracene-2-carboxamide (**1i**) were investigated. In contrast to anthracene (**1a**), **1b**, and **1c**, the 2-methoxy-substituted anthracene derivatives **1d–1h** exhibit two emission lifetimes. The determination of the lifetimes at different emission wavelengths and additional time-resolved emission spectroscopy (TRES) reveal that the dual emission originates from two different, interconvertible emissive species, with the *s*-cis and *s*-trans conformation relative to the exocyclic C2–O bond. The energy difference between the two emissive species is very small (<0.1 eV) both in the ground and in the excited state. The larger energy difference between the conformers in the excited-state is responsible for the interconversion within the singlet excited-state lifetimes of the *s*-cis into the *s*-trans conformations leading to coupled decay kinetics. The proposed mechanism for the dual emission was qualitatively supported by theoretical studies on CASSCF and DFT level. In addition, the emission lifetimes of the fluoride- and pH-sensitive fluorescent probes **1f** and **1g** change upon addition of fluoride or acid, respectively, so that in these cases the detection of the fluorescence lifetime may be used complementary to the steady-state fluorimetric detection of these analytes.

## Introduction

Organic fluorescent probes are among the most powerful tools in analytical biology and medicine because they allow the detection of analytes with high selectivity and sensitivity.<sup>1</sup> As a consequence, the number of tailor-made fluorescent probes that are designed for the detection of particular analytes has increased dramatically during the past decade. Most fluorescent probes indicate the presence of an analyte by a change of their steady-state emission properties. Upon interaction of the analyte with the fluorescent probe, the emission intensity or the emission color, in particular the wavelength of the emission maximum, change significantly. Thus, a drastic increase of the emission intensity (light-up probes) and a significant shift of the emission maximum upon interaction with the analyte are sufficient indicators; however, fluorescence quenching does not appear to be an appropriate tool for selective detection, because the quenching may also be caused by several other external factors. Other artifacts, such as fluctuations of the excitation source, inner filter effects, or light scattering, may lead to inherent errors of the steady-state emission data and may, in the worst case, provide misleading data.<sup>2</sup> Moreover, the concentration of the sample is a crucial parameter, when the signal intensity is used

for analyte detection. The emission lifetime, however, is less affected by these parameters and even tolerates small amounts of nonfluorescent impurities. Thus, the so-called lifetime-based sensing represents a method that may be used for efficient and unambiguous fluorimetric detection.<sup>3</sup> Along these lines, cation-sensitive fluorescent probes, especially pH sensors, have been investigated in detail,<sup>4</sup> whereas relatively few examples have been reported for the lifetime-based anion sensing.<sup>5</sup>

We have recently shown that the 2-(6-methoxyanthr-2-yl)-4,4-dimethyl-2-oxazoline (**1g**) and the 2-(6-methoxyanthr-2-yl)-pyridine (**1h**) are pH-sensitive fluorescence probes, since the protonation of the heterocyclic moieties increases their acceptor properties and results in significant red-shifts of the absorption and emission maxima of the conjugated anthracene chromophore.<sup>6</sup> On the other hand, the emission maxima of the acylureidoanthracene derivative **1f** in acetonitrile are blue-shifted by 50 nm upon addition of fluoride.<sup>7</sup> Thus, both systems may be used for ratiometric steady-state sensing. During our ongoing studies of the properties of these fluorescent probes, we wished to explore the ability of these compounds to be used for lifetime-based sensing of cations and ions. Much to our surprise, time-resolved experiments revealed a dual fluorescence of compounds **1f–1h** even in the absence of an analyte. In this article we present our studies to explain this phenomenon, which may interfere with the intended lifetime-based sensing, and we will demonstrate that the dual lifetime is an intrinsic property of the 2-methoxyanthracene fluorophore.

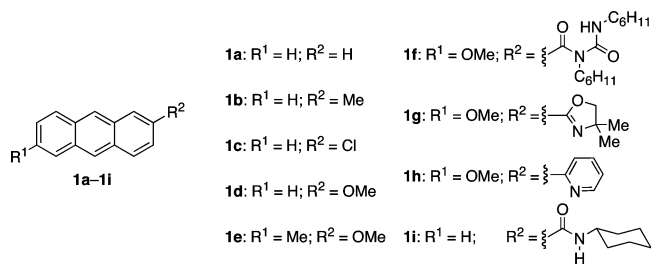
\*Corresponding authors. E-mails: bohne@uvic.ca; ihmels@chemie.uni-siegen.de.

<sup>†</sup> University of Siegen, Physical and Theoretical Chemistry.

<sup>‡</sup> University of Victoria.

<sup>§</sup> University of Siegen, Organic Chemistry II.

<sup>||</sup> University of Cologne.



## Experimental

**Materials.** Tetra(*n*-butyl)ammonium fluoride, 1 M in THF (Acros, cont. 5% of H<sub>2</sub>O), sodium dodecyl sulfate (SDS, Sigma, > 99%), acetonitrile (Caledon, 99.8%), chloroform (EM, HPLC grade), cyclohexane (Caledon, spectrograde), and methanol (ACP, spectrograde) were used as received. Compound **1a** (Aldrich, zone refined, > 99%) was used as purchased, and compounds **1b** and **1c** (Aldrich) were purified by recrystallization. Anthracene derivatives **1d–h** were synthesized according to published procedures.<sup>8</sup> The purity of the anthracene derivatives was checked by HPLC and GC, showing purities greater than 99.5%.

***N*-Cyclohexylanthracene-2-carboxamide (1i).** A suspension of anthracene-2-carboxylic acid (111 mg, 500  $\mu$ mol) in anhyd. benzene (5 mL) was treated with SOCl<sub>2</sub> (0.50 mL) and heated under reflux for 12 h. After cooling to room temp. the solution was filtered through a paper filter to remove the small amount of tar, and all volatile components were removed in vacuum; the remaining yellow solid was dissolved in anhyd. benzene (5 mL) and evaporated to dryness once again. The residue was dissolved in anhyd. benzene (5 mL), and cyclohexylamine (250  $\mu$ L, 217  $\mu$ g, 2.19 mmol) in anhyd. benzene (1 mL) was added at 0 °C. The reaction mixture was stirred for 1 h at room temp. and 1 h under reflux, while a beige precipitate separated. After cooling, the solvent was removed in vacuum, and the residue was dissolved in CHCl<sub>3</sub> (25 mL) and washed with 1 M aq. HCl, water, 0.5 M NaOH and water (20 mL each). The organic layer was dried with Al<sub>2</sub>O<sub>3</sub> and evaporated in vacuum. The residue was recrystallized from pyridine to give analytically pure **1i** (42 mg, 28%) as fine pale-yellow needles, mp 270–272 °C. <sup>1</sup>H NMR (400 MHz, CDCl<sub>3</sub>–CF<sub>3</sub>COOD):  $\delta$  1.21–1.49 (m, 5 H), 1.69–1.73 (m, 1 H), 1.80–1.85 (m, 2 H), 2.10–2.13 (m, 2 H), 4.03–4.08 (m, 1 H), 6.52 (br s, 1 H, NH), 7.51–7.57 (m, 2 H), 7.65 (d, <sup>3</sup>*J* = 9 Hz, 1 H), 8.02–8.08 (m, 2 H), 8.46 (br s, 2 H), 8.54 (s, 1 H). <sup>13</sup>C NMR (100 MHz, CDCl<sub>3</sub>–CF<sub>3</sub>COOD):  $\delta$  24.7 (2 CH<sub>2</sub>), 25.3 (CH<sub>2</sub>), 32.9 (2 CH<sub>2</sub>), 50.2 (CH), 121.8 (CH), 126.2 (CH), 126.5 (CH), 126.8 (CH), 128.2 (CH), 128.4 (CH), 128.5 (CH), 129.3 (CH), 129.4 (C<sub>q</sub>), 129.5 (CH), 130.1 (C<sub>q</sub>), 132.2(C<sub>q</sub>), 132.3(C<sub>q</sub>), 133.1(C<sub>q</sub>), 169.8 (CO). Elemental anal. calcd for C<sub>21</sub>H<sub>21</sub>NO (303.4): C, 83.13; H, 6.98; N, 4.62. Found: C, 83.10; H, 6.93; N, 4.70.

The fluorescence experiments were performed in quartz cells (*l* = 1 cm) capped with pre-washed rubber septa. Solutions were deoxygenated by bubbling nitrogen for at least 20 min. Concentrations for **1b** and **1d–1h** were determined from absorption measurements [**1b** (MeOH),  $\epsilon_{377} = 3614 \text{ cm}^{-1} \text{ M}^{-1}$ ; **1d** (MeOH),  $\epsilon_{391} = 2359 \text{ cm}^{-1} \text{ M}^{-1}$ ; **1e** (MeOH),  $\epsilon_{392} = 3040 \text{ cm}^{-1} \text{ M}^{-1}$ ,  $\epsilon_{345} = 3500 \text{ cm}^{-1} \text{ M}^{-1}$ ; **1f** (MeOH),  $\epsilon_{393} = 3832 \text{ cm}^{-1} \text{ M}^{-1}$ ; **1g** (MeOH),  $\epsilon_{395} = 4074 \text{ cm}^{-1} \text{ M}^{-1}$ ; **1h** (MeOH),  $\epsilon_{398} = 5012 \text{ cm}^{-1} \text{ M}^{-1}$ ; **1i**,  $\epsilon_{385} = 3296 \text{ cm}^{-1} \text{ M}^{-1}$ ]. Solutions for **1a** and **1c** were prepared from concentrated stock solutions. The 0.1 M SDS solution was prepared with deionized water (Sybron-Barnstead system,  $\geq 17.8 \text{ M}\Omega \text{ cm}^{-1}$ ). Compound **1g** and **1h** were protonated by addition of 2  $\mu$ L of a 10 M HCl

aqueous solution to 2 mL of solution **1g** and **1h** in methanol and chloroform (pH  $\sim$ 2), respectively. Titration experiments of **1f** with fluoride were performed by the addition of *n*-Bu<sub>4</sub>N<sup>+</sup>F<sup>–</sup> (1 M in THF) to a solution of **1f** in acetonitrile. When small amounts were added (fluorescence lifetime measurements), no correction for dilution of **1f** was made. For fluorimetric titration of fluoride to **1f**, however, both the analyte and the titrant solution contained the same concentration of **1f** to avoid the dilution effect.

**Equipment.** HPLC experiments were performed on a Varian Autosampler 9100 with a Varian 9012 pump and J&M Tidas detector; stationary phase Macherey-Nagel EC 250/4 Nucleodur 100–5 C18 ec-column (length: 250 mm, inner diameter: 4 mm), eluent acetonitrile/water mixture, the latter contained 0.1% trifluoroacetic acid; gradient 80% CH<sub>3</sub>CN, 20% H<sub>2</sub>O at *t* = 0; 100% CH<sub>3</sub>CN at *t* = 10 min. GC experiments were performed on a Fisons 8000 GC using a DB-1 column.

Absorbance spectra were measured on a Cary 1 spectrophotometer. Steady-state fluorescence spectra were collected with a Varian Eclipse spectrofluorimeter at a right-angle sample orientation in quartz sample cells (path length *l* = 1 cm) or with a PTI QM-2 fluorimeter; in both cases the samples were kept at constant temperature (20.0  $\pm$  0.2 °C), with the exception of low-temperature studies. For experiments at 77 K, a 2 mm (internal diameter) cylindrical quartz cell containing the compound in toluene was slowly immersed into a custom-built quartz Dewar (internal dimension of 10  $\times$  10 mm) containing liquid nitrogen. The emission and excitations slits on the monochromators were set such that their bandwidths were 2 nm for all experiments.

Time-resolved fluorescence decays were measured with an Edinburgh OB 920 single-photon-counting system. The excitation source was a hydrogen filled lamp. The instrument response function (IRF) was collected with a Ludox (Aldrich) solution. The samples were kept at constant temperature using Lauda RM6 circulating bath (20.0  $\pm$  0.2 °C), with the exception of temperature dependence studies. The emission and excitation slits were set such that the bandwidths were 16 nm (maximum slit width). The count rate for the samples and IRF runs was kept below 1000 counts/s, and in the case of the IRF the iris between the excitation lamp and sample was used to decrease the count rate when necessary. Decays were collected at fixed wavelengths and the maximum number of counts ranged between 2000 and 10 000 counts. Control experiments showed that the lifetimes recovered from multiexponential fits were the same when the maximum number of counts was 2000 or 10 000. The decay curves were analyzed using the Edinburgh software where the IRF was deconvoluted from the decay of the fluorophore. A nonlinear least squared method was employed for the fit of the decay to a sum of exponentials. The value of  $\chi^2$  (0.9 to 1.2), and a visual inspection of the residuals and the autocorrelation function were used to determine the quality of the fit. Time-resolved emission spectra (TRES) were collected by setting a constant collection time (20–60 min) for each wavelength. The decays were collected at wavelength intervals of 10 or 15 nm.

**Calculations.** As a starting point a geometry optimization for compound **1d** was performed employing the RI-DFT method with the B-P86 functional and a cc-pVTZ basis set using the program package TURBOMOLE.<sup>9</sup> Subsequently the optimized result was used to generate the data for each conformation by rotating the methoxy group by a dihedral angle  $\alpha$  around the O–C2 axis out of the anthracene plane. This angle was changed in steps of 10 degrees, resulting in 19 different structures to be

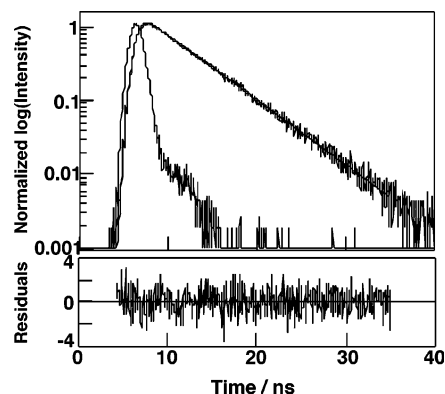


**Figure 1.** Fluorescence decay of **1b** in methanol ( $[1b] = 1.4 \times 10^{-4}$  M,  $\lambda_{ex} = 250$  nm,  $\lambda_{em} = 400$  nm) and the IRF. The solid line corresponds to the fit of the decay to a monoexponential function. The residuals between the experimental data and the fit are shown in the lower panel.

calculated. For each calculation a standard Hartree–Fock (HF) calculation with a cc-pVDZ basis set using the program package MOLPRO was performed,<sup>10</sup> which was also used in all subsequent steps. In accordance with the results of Kawashima et al. obtained for the parent anthracene,<sup>11</sup> the *p*-functions on the hydrogen atoms were omitted, as they were shown to be of no importance for the calculation of optical transitions. In order to find the optical transition energies, the energies of the ground state and first excited-state were obtained from a Complete Active Space Self-Consistent Field (CASSCF) calculation. A maximum of 13 active orbitals were selected in each case, including the 8 occupied valence orbitals and the most relevant 5 virtual orbitals of the  $\pi$  system resulting from the HF step. During the CAS step both the coefficients of the active space wave functions and the wave functions themselves were optimized. This procedure requires extensive computer time and yields a reliable procedure for energy determinations.

## Results

The objective of performing time-resolved fluorescence experiments for compounds **1f–1h** was to obtain mechanistic information that could be employed to enhance their usefulness as fluorescence probes for potential applications such as selective ion sensing. Preliminary single photon counting experiments with **1g** and **1f** showed that the fluorescence decay did not follow a monoexponential function. To understand this observation, control experiments were performed with model compounds **1a–1e**.

The fluorescence decays were collected at three wavelengths. One wavelength was close to the maximum in the fluorescence spectra, while the other two wavelengths were either at shorter or longer wavelengths when compared to the wavelength for maximum emission. A compromise had to be found between how much we could shift the wavelengths and the time required for the collection of the decay, because this time increases as the emission intensity decreases. It is important to note that the bandwidth for the single photon counting experiments was 16 nm and therefore a wide range of wavelengths was collected. For **1a–1c** the emission decays were monoexponential at all wavelengths (Figure 1, Table 1).

For compounds **1d** and **1e**, which contain a methoxy substituent in the 2-position, the fluorescence decay was monoexponential only at the wavelength close to the maximum emission. At shorter wavelengths a fast decay was observed followed by a long-lived decay, while at longer wavelengths

**TABLE 1: Emission Lifetimes of Anthracene Derivatives 1a–1e<sup>a</sup>**

compd	solvent	$\tau_1$ /ns	$\tau_2$ /ns
<b>1a<sup>b</sup></b>	CH <sub>3</sub> OH	5.4 ± 0.1	
<b>1b<sup>c</sup></b>	CH <sub>3</sub> OH	4.5 ± 0.1	
<b>1c<sup>c</sup></b>	CH <sub>3</sub> OH	3.5 ± 0.1	
<b>1d<sup>d</sup></b>	CH <sub>3</sub> OH	24.7 ± 0.6	3.5 ± 0.4
<b>1d<sup>d</sup></b>	CH <sub>3</sub> CN	26.4 ± 0.1	5.4 ± 0.3
<b>1d<sup>e</sup></b>	C <sub>6</sub> H <sub>6</sub>	21.1 ± 0.1	2.6 ± 0.1
<b>1e<sup>d</sup></b>	CH <sub>3</sub> OH	24 ± 2	3.6 ± 0.4
<b>1e<sup>d</sup></b>	CH <sub>3</sub> CN	25.7 ± 0.3	5.3 ± 0.8
<b>1e<sup>e</sup></b>	C <sub>6</sub> H <sub>6</sub>	20.3 ± 0.1	2.7 ± 0.2

<sup>a</sup> Errors are standard deviations, fitting parameters for individual decays are shown in the SI. <sup>b</sup>  $\lambda_{ex} = 250$  nm,  $\lambda_{em} = 370, 400,$  or  $445$  nm,  $[1a] = 6.8 \mu\text{M}$ . <sup>c</sup>  $\lambda_{ex} = 250$  nm,  $\lambda_{em} = 375, 400,$  or  $450$  nm,  $[1b] = 0.14$  mM,  $[1c] = 19 \mu\text{M}$ . <sup>d</sup>  $\lambda_{ex} = 260$  nm,  $\lambda_{em} = 400, 420,$  or  $480$  nm,  $[1d] = 15 \mu\text{M} - 0.5$  mM,  $[1e] = 6.1 \mu\text{M} - 0.15$  mM. <sup>e</sup>  $\lambda_{ex} = 260$  nm,  $\lambda_{em} = 400, 425,$  or  $480$  nm,  $15 \mu\text{M}$ .

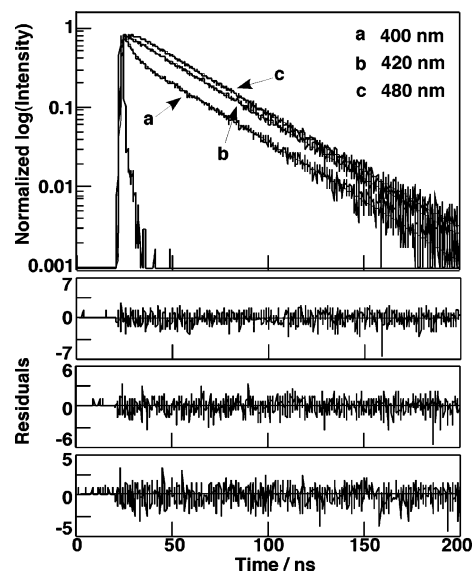


**Figure 2.** Fluorescence decays of **1d** in methanol ( $16 \mu\text{M}$ ,  $\lambda_{ex} = 260$  nm) collected at several emission wavelengths (a, 400 nm; b, 420 nm; c, 480 nm) and the IRF. The solid lines correspond to the fits of the experimental data to a monoexponential function at 420 nm and the sum of two exponentials at 400 and 480 nm. The residuals between the data and the fits are shown in the panels below the main figure (top, 400 nm; middle, 420 nm; bottom, 480 nm).

an initial growth kinetics was observed (Figure 2). The decays at the long and short wavelengths were fit to the sum of two exponentials and the lifetimes for the fast and slow components were the same for both decays. In addition, the lifetime for the monoexponential decay observed at the wavelength for the emission maximum was the same as the lifetimes for the long-lived component at the other two wavelengths. Both emitting species were quenched by oxygen. Based on the lifetimes in aerated and de-aerated solutions, the oxygen quenching is diffusion controlled. The lifetimes and pre-exponential factors did not change when the concentrations of **1d** and **1e** were raised from  $16 \mu\text{M}$  to  $0.5$  mM and  $6.1 \mu\text{M}$  to  $0.15$  mM, respectively, suggesting that the dual lifetimes were not due to an artifact because of aggregation of the chromophores. The lifetimes for **1d** and **1e** were measured in methanol, acetonitrile and cyclohexane (Table 1). Both lifetimes for **1d** and **1e** are the same in each solvent, with the longest lifetimes being observed in acetonitrile, followed by methanol and cyclohexane.

TRES experiments were performed to collect the spectra at different delays after the excitation pulse. A red shift in the emission spectrum was observed at the longer delays

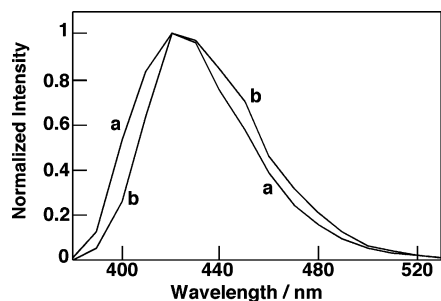


**Figure 3.** Time-resolved emission spectra (TRES) of **1d** in methanol ( $5 \times 10^{-4}$  M,  $\lambda_{\text{ex}} = 260$  nm) integrated between delays after the onset of the emission of 0 and 10 ns (a) and between delays of 40 and 90 ns (b).

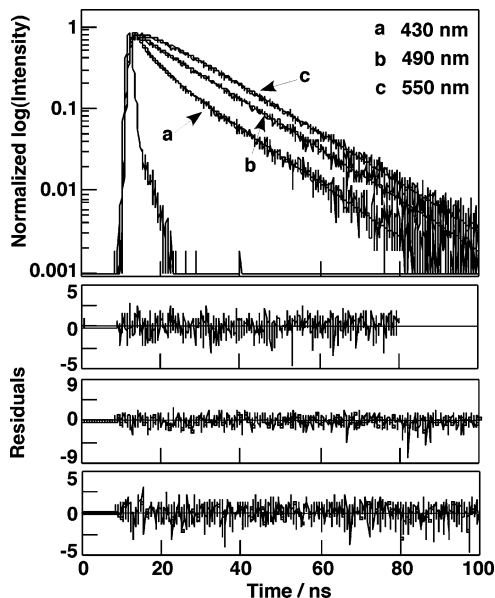


**Figure 4.** Fluorescence decays of **1f** in acetonitrile ( $5.8 \mu\text{M}$ ,  $\lambda_{\text{ex}} = 280$  nm) collected at several emission wavelengths (a, 430 nm; b, 490 nm; c, 550 nm) and the IRF. The solid lines correspond to the fit of the experimental data to the sum of two exponentials. The residuals between the data and the fits are shown in the panels below the main figure (top, 430 nm; middle, 490 nm; bottom, 550 nm).

(Figure 3, for **1d**). This result indicates that the short-lived species has a slightly higher energy than the long-lived species. An exact energy difference cannot be calculated because the spectrum at short delays is a composite spectrum for the two species. In addition, the spectra are not resolved because of the 16 nm bandwidth used in the single photon counting experiments. These experiments reveal that the two lifetimes are an intrinsic feature of the 2-methoxyanthracene chromophore.

The fluorescence of **1f** was previously shown to have a very strong solvatochromic effect, i.e., the fluorescence emission maxima are significantly red-shifted with increasing acceptor numbers of the solvent ( $\lambda_{\text{max}} = 453$  nm in cyclohexane,  $\lambda_{\text{max}} = 487$  nm in acetonitrile and  $\lambda_{\text{max}} = 534$  nm in methanol). The emission quantum yields are only slightly influenced by the nature of the solvent ( $\phi_{\text{fl}} = 0.54$  in cyclohexane,  $\phi_{\text{fl}} = 0.64$  in acetonitrile and  $\phi_{\text{fl}} = 0.44$  in methanol).<sup>7</sup> The fluorescence decay for **1f** in all three solvents followed a non-exponential function at all wavelengths, including the decay at the emission maximum (Figure 4, Table 2). The lifetimes for the long-lived component for **1f** in cyclohexane and acetonitrile were the same, whereas this lifetime was shorter in methanol. In the case of the short-lived component, the same lifetimes were observed in methanol

**TABLE 2: Emission Lifetimes of 1f–1h in Various Solvents and in the Absence and Presence of Analytes<sup>a</sup>**

compd	solvent	$\tau_1/\text{ns}$	$\tau_2/\text{ns}$
<b>1f</b> <sup>b,c</sup>	MeOH	$8.4 \pm 0.3$	$3.1 \pm 0.7$
<b>1f</b> <sup>b,d</sup>	C <sub>6</sub> H <sub>12</sub>	$12.3 \pm 0.2$	$1.3 \pm 0.4$
<b>1f</b> <sup>b,e</sup>	CH <sub>3</sub> CN	$12.5 \pm 0.8$	$4 \pm 1$
<b>1f-R</b> <sup>b,f</sup>	CH <sub>3</sub> CN	$17.8 \pm 0.2$	$5.3 \pm 0.2$
<b>1g</b> <sup>g,h</sup>	MeOH	$13 \pm 1$	$3.5 \pm 0.5$
<b>1g-H</b> <sup>+g,i</sup>	MeOH	$8.7 \pm 0.7$	$2.9 \pm 0.3$
<b>1g</b> <sup>g,j</sup>	SDS/H <sub>2</sub> O	12.5	3.7
<b>1h</b> <sup>k,l</sup>	MeOH	$8.4 \pm 0.1$	$2.6 \pm 0.3$
<b>1h</b> <sup>k,m</sup>	CHCl <sub>3</sub>	$6.3 \pm 0.2$	$2.0 \pm 0.4$
<b>1h-H</b> <sup>+n</sup>	CHCl <sub>3</sub>	$6.1 \pm 0.2$	$1.8 \pm 0.3$

<sup>a</sup> Errors are standard deviations, fitting parameters for individual decays can be found in the SI. <sup>b</sup>  $\lambda_{\text{ex}} = 280$  nm, [**1f**] =  $5.8 \mu\text{M}$ . <sup>c</sup>  $\lambda_{\text{em}} = 450, 530, \text{ or } 620$  nm. <sup>d</sup>  $\lambda_{\text{em}} = 410, 440, \text{ or } 500$  nm. <sup>e</sup>  $\lambda_{\text{em}} = 430, 490, \text{ or } 550$  nm. <sup>f</sup>  $\lambda_{\text{em}} = 400, 440, \text{ or } 510$  nm,  $[\text{F}^-] = 1.5$  mM. <sup>g</sup> [**1g**] =  $5.0 \mu\text{M}$ . <sup>h</sup>  $\lambda_{\text{ex}} = 280$  or  $380$  nm,  $\lambda_{\text{em}} = 410, 440, \text{ or } 510$  nm. <sup>i</sup>  $\lambda_{\text{ex}} = 290$  or  $310$  nm,  $\lambda_{\text{em}} = 490, 500, 540, \text{ or } 580$  nm, pH  $\sim 2$  (addition of aq. HCl). <sup>j</sup> SDS = sodium dodecyl sulfate, [SDS] =  $0.1$  M;  $\lambda_{\text{ex}} = 290$ ,  $\lambda_{\text{em}} = 440$  nm. <sup>k</sup> [**1h**] =  $5.2 \mu\text{M}$ . <sup>l</sup>  $\lambda_{\text{ex}} = 280$  nm,  $\lambda_{\text{em}} = 410, 440, \text{ or } 510$  nm. <sup>m</sup>  $\lambda_{\text{ex}} = 290$  nm,  $\lambda_{\text{em}} = 410, 440, \text{ or } 480$  nm. <sup>n</sup>  $\lambda_{\text{ex}} = 320$  nm,  $\lambda_{\text{em}} = 490, 530, \text{ or } 600$  nm, pH  $\sim 2$ .

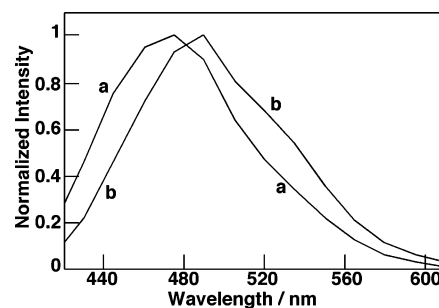


**Figure 5.** Time-resolved emission spectra (TRES) of **1f** in acetonitrile ( $6.8 \mu\text{M}$ ,  $\lambda_{\text{ex}} = 280$  nm) integrated between delays after the onset of the emission of 0 and 10 ns (a) and between delays of 40 and 90 ns (b).

and acetonitrile, while the short-lived component was significantly shorter in cyclohexane. The TRES for **1f** in acetonitrile showed a larger shift in the emission spectra with the delay after excitation (Figure 5) than that observed for **1d**. This result is consistent with the fact that a non-exponential decay was observed for **1f** at its fluorescence maximum.

The strong solvatochromic effect observed for the fluorescence spectra of **1f** is due to the stabilization of the excited state in solvents with high acceptor number.<sup>7</sup> The hydrogen bonding to the carbonyl moiety adjacent to the aromatic ring plays an additional role in the photophysics of **1f**. When the intramolecular hydrogen bonding is disrupted by the addition of analytes, such as fluoride, in solvents with high acceptor numbers, a marked blue shift of the emission maximum is observed to wavelengths close to those observed in solvents with low acceptor numbers such as cyclohexane.<sup>7</sup>

A fluorimetric titration of fluoride to **1f** was performed (Figure 6) to establish the fluoride concentration at which all **1f** was bound ( $>1$  mM). The isoemissive point observed suggests that two species of **1f**, the free and fluoride-bound ones, were present in solution. A concentration of  $1.5$  mM fluoride was employed for the single photon counting experiments. The fluorescence decay was adequately fit to the sum of two exponentials and the addition of fluoride led to a marked increase of the lifetime for the long-lived component (Table 2). TRES experiments also revealed the existence of two emissive species (cf. Supporting Information).

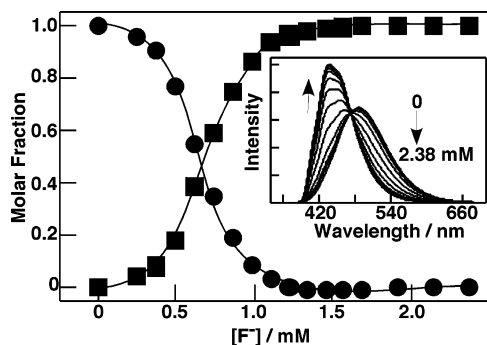


**Figure 6.** Spectrofluorimetric titration of **1f** ( $10^{-5}$  M in acetonitrile) with  $\text{Bu}_4\text{N}^+\text{F}^-$  measured at 488 nm (●, free **1f**) and 438 nm (■, bound **1f**). The inset shows the emission spectra at various fluoride anion concentrations.

To check whether the blue shift of the emission maximum and the increase of the emission lifetime of **1f** upon addition of fluoride are characteristic properties of the acylureido functionality and its interplay with the anthracene fluorophore and not solely the effect of the fluoride-bound amide functionality, the anthracene-2-carboxamide **1i** was investigated as a reference compound. The methoxy group in the 6-position was omitted to avoid the dual lifetimes. The amide **1i** exhibits the usual emission properties of anthracene derivatives ( $\lambda_{\text{fl,max}} = 418$  nm), and the emission maximum and fluorescence intensity do not change upon addition of fluoride ions (cf. Supporting Information). Moreover, the average lifetime for **1i** in acetonitrile is  $6.7 \pm 0.1$  ns, and this lifetime remains unchanged ( $6.5 \pm 0.1$  ns) upon addition of tetrabutylammonium fluoride.

Compounds **1g** and **1h** show pH-sensitive emission spectra, i.e., a red shift of the emission is observed when the oxazoline and pyridine moieties are protonated. The emission maximum upon protonation shifted from 450 to 544 nm for **1g** in methanol and from 443 to 540 nm for **1h** in chloroform.<sup>6</sup> Both compounds showed dual lifetimes in the protonated and unprotonated forms (Table 2, see decays in Supporting Information). In the case of **1g**, a decrease of the long-lived component was observed when the fluorophore was protonated, whereas no changes in the lifetimes were observed for **1h**.

Further control experiments were performed with **1g**. The same lifetimes and pre-exponential factors were observed for the fluorescence decay of **1g** in methanol when excited at 280 or 380 nm. These excitation wavelengths correspond to different absorption bands of **1g**. To further rule out the possible aggregation of the fluorophores, the lifetimes for **1g** were measured in sodium dodecyl sulfate (SDS) micelles, which were likely to break up any aggregates since the micellar concentration was much higher than that of **1g**. The same lifetimes and pre-exponential factors were obtained in methanol and SDS micelles (cf. Supporting Information). This experiment rules out the possibility of aggregate formation because even if some aggregates were present, the relative amount with respect to the monomer concentration should be different in methanol and SDS micelles leading to different pre-exponential factors. Finally, the excitation spectra for the fluorescence of **1g** at 77 K in toluene were recorded when the fluorescence was detected at 400 and 460 nm. At low temperature a small shift of 2 nm to longer wavelengths was observed for the peak maxima when the emission was detected at 460 nm (cf. Supporting Information). This observation is in line with the small shifts observed for the spectra in the TRES experiment.

In order to further elucidate the origin of the two fluorescent species detected experimentally, a theoretical investigation of

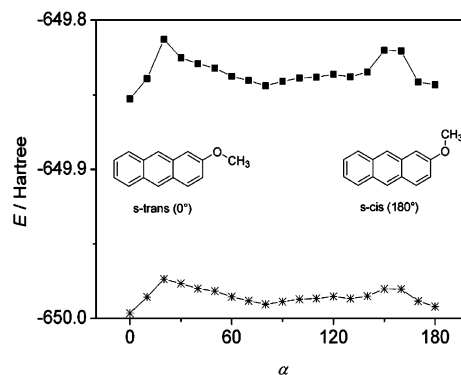


**Figure 7.** Ground-state energies (solid line, stars) and first excited-state energies (solid line, squares) of methoxyanthracene (**1d**) for various rotation angles  $\alpha$ . The molecule is plotted for 0 and 180 degrees, showing how the methoxy group was rotated ( $0^\circ = s\text{-trans}$ ,  $180^\circ = s\text{-cis}$ ).

compound **1d** was conducted. We propose below that the different emissive species correspond to different excited-state conformations that result from the rotation of the methoxy group relative to the anthracene plane. This proposal is the same as previously suggested for 2-vinylanthracene derivatives<sup>12</sup> and *N*-methoxy-1-(2-anthryl)ethanimine,<sup>13</sup> where dual fluorescence with coupled processes were observed. To check this assumption we calculated the energies of the conformers that result from a variation of the dihedral angle ( $\alpha = \text{C1-C2-O-C}_{\text{Me}}$ ) between 0 and 180 degrees, where  $0^\circ$  correspond to the conformation in which the methyl group points along the C2–C3 bond (*s-trans*) and  $180^\circ$  refers to the conformation in which the methyl group is next to the hydrogen atom at C1 (*s-cis*; see inset in Figure 7). In Figure 7 the change of both the ground-state and first excited-state energies with respect to the rotation angle  $\alpha$  are shown.

The ground state of the system was located at  $0^\circ$ , while the conformer at  $180^\circ$ , i.e., with the methoxy group bent outward, is slightly higher in energy by 0.12 eV (12 kJ/mol). The rotational barriers for both electronic states are defined by the peaks at 20 degrees, where the barrier for the ground state was calculated to be 0.62 eV (60 kJ/mol) and the barrier for the excited-state was calculated to be 1.09 eV (105 kJ/mol). The energy difference for the  $S_0$  and  $S_1$  states at  $0^\circ$  was calculated to be 3.91 eV (378 kJ/mol), whereas the energy difference for the  $S_0$  and  $S_1$  states at  $180^\circ$  was calculated to be 4.05 eV (391 kJ/mol). As a consequence, the conformer at  $180^\circ$  in the excited state is less stable by 0.26 eV (25 kJ/mol) compared to the conformer at 0 degrees. From the qualitative point of view these calculations indicate that in the excited state the equilibrium between the conformers at  $180^\circ$  and  $0^\circ$  is different from that in the ground state, and in the excited state the conformer at  $0^\circ$  is favored. As a consequence, the energy for the emission of the conformer at  $0^\circ$  is lower than the energy for the emission of the conformer at  $180^\circ$ .

Two discrepancies are present in the CASSCF calculations. The energy calculated for the  $S_0 \rightarrow S_1$  transition is overestimated, which is a consequence of the approximation inherent to CASSCF. This effect is commonly observed,<sup>14</sup> and the only important point for the experiments reported is that a shift in the emission wavelength is predicted. The energy shift cannot be measured from the experimental data because the fluorescence spectra at short delays are combinations of the spectra of the different conformers.

The second discrepancy is the height of the rotational barriers at  $20^\circ$  in the ground and excited states. While the CASSCF

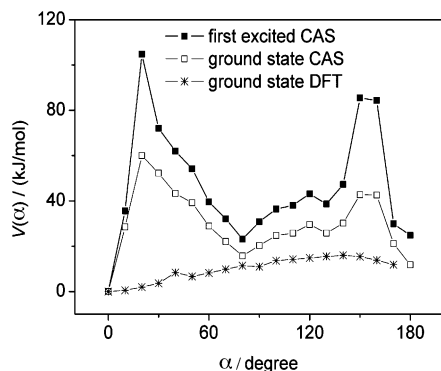


**Figure 8.** Ground-state energy (empty squares) and first excited-state energy (filled squares) of the **1d** system for various rotation angles  $\alpha$  as obtained with the CASSCF method. All curves are taken to start at zero at the  $\alpha = 0$  position. For comparison DFT results for the ground state using the B3LYP level are also included (stars).

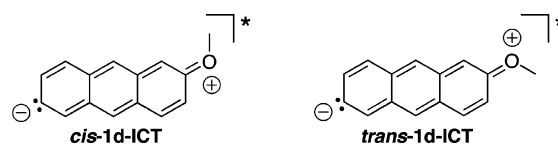
approach is the method of choice for complex conjugated systems, the active space encountered in our calculations appears to be at the limit of what can be handled at present. The inevitable selection of active orbitals to be included in the calculation, as well as the mere size of the numerical iterations, seem to lead to rotation barriers which might be artifacts to a large extent. This is illustrated in Figure 8, where all potential curves are taken to start at zero for the  $\alpha = 0$  position for the sake of comparison. In the case of the CASSCF calculations, both the ground-state potential curve and the one for the first excited-state display rotation barriers between 40 and 60 kJ/mol (ground state) or 80 and 105 kJ/mol (excited state) at dihedral angles  $\alpha$  of approximately  $20^\circ$  and  $150^\circ$ ; however, these values are certainly too large, in particular when compared to the rotational barrier that has been calculated for anisole (ca. 12 kJ/mol).<sup>15</sup> Therefore, we performed complementary calculations with a density functional theory (DFT) ground-state calculation for the same geometrical structures employing a B3LYP functional and a 6-311+G\*\* basis. The result of this calculation is presented in Figure 8 and is significantly different from the data of the CASSCF calculation. The maximum is found at  $140^\circ$  and turns out to be significantly smaller in energy. On the other hand, the DFT results cannot provide information about the excited-state potential energy curve for conjugated systems. The reason for this shortcoming of DFT is that this is a theory to describe the ground state and it cannot predict excited states of any kind. This failure is particularly pronounced for states of a multi-determinant nature such as the one presented here.<sup>16</sup> Considering the particular inherent limitations of each theoretical method, we assume that the real potential curve of the ground state is located between the ones resulting from the CASSCF and the DFT calculations. Nevertheless, independent of these limitations, both methods are remarkably consistent regarding the energy difference between the two ground-state conformers of 2-methoxyanthracene at  $\alpha = 0^\circ$  and  $180^\circ$ .

To further probe the existence of an energy barrier for the interconversion between the two emitting species the lifetimes for **1d** were measured at 400, 425 and 480 nm at  $10^\circ$ ,  $20^\circ$ ,  $45^\circ$ , and  $60^\circ$  C (cf. Supporting Information). The long-lived component did not vary with temperature, while the short-lived component became shorter at higher temperatures. A barrier of 19 kJ/mol was estimated from these measurements. It is important to note that the temperature range studied is narrow because we could not measure decays at temperatures below  $10^\circ$  C and the short decay reached the time resolution of our equipment at the highest temperature investigated.

## Discussion

During our attempts to extend the potential application of the fluorescent probes **1f–1h** toward lifetime based sensing, we encountered a feature of these anthracene derivatives, namely the appearance of two different fluorescent species with significantly different lifetimes, that were present even in the absence of an analyte. To assess the origin of this dual fluorescence, the substitution pattern of the anthracene derivatives was varied systematically, and this study demonstrated that the anthracene derivatives with a methoxy substituent in the 2-position exhibit dual fluorescence. It should be noted that artifacts such as impurity emissions and aggregation of the fluorophore were eliminated. The high degree of purity of the samples was determined in GC and HPLC experiments, and the lifetimes and pre-exponential factors were the same when the excitation wavelength and the concentrations of the fluorophore were varied.

In general, three mechanisms may be considered as the origin for the dual lifetimes of methoxyanthracene derivatives. (a) Upon irradiation, two different transitions take place that lead to two independent excited states. Both excited states are deactivated by fluorescence, however, with significantly different emission rates. (b) In the excited-state an intramolecular charge transfer (ICT) from the methoxy functionality to the anthracene ring gives the two isomeric intermediates *cis-1d-ICT* and *trans-1d-ICT* that may emit at different wavelengths and with different fluorescence lifetimes. Note that these resonance forms may also be considered for the ground state, however, after ICT these resonance forms contribute much more to the overall electron distribution than in the ground state. In



the ICT excited state, configurational isomers are formed (*cis-1d-ICT* and *trans-1d-ICT*) with different emission properties, in particular different fluorescence lifetimes. (c) Methoxyanthracene derivatives exist in two different conformations in the ground and excited state. These conformations have different energies and are separated by a significant energy barrier. Thus, the two emission rates are the result of equilibrating conformers with different fluorescence lifetimes.

Usually, the first excited state of anthracene,  $S_1$ , is assigned to a  ${}^1L_a$  transition with the transition dipole moment oriented along the short axis of the molecule.<sup>17</sup> Nevertheless, experimental and theoretical studies reveal a  ${}^1L_b$  transition with a similar transition energy, but with a very small oscillator strength.<sup>18</sup> Thus, for anthracene the energy of the  ${}^1L_a$  state was determined to be between 3.31 and 3.43 eV, whereas the  ${}^1L_b$  transition has an energy between 3.45 and 3.84 eV.<sup>19</sup> The two first singlet excited states for 2-methoxyanthracene are strongly mixed and the energies of the first two excited states were determined to be 3.16 eV ( $25,510\text{ cm}^{-1}$ , 392 nm) and 3.57 eV ( $28,820\text{ cm}^{-1}$ , 347 nm).<sup>20</sup> These data show clearly that the dual emission of methoxyanthracene is not due to the population of the  ${}^1L_b$  state, because the observed energy difference between the two emissive species, as obtained from the TRES experiments, is very small ( $<0.1\text{ eV}$ ) and does not match the energy difference between the  ${}^1L_a$  and  ${}^1L_b$  state. Moreover, as it has been shown that the  ${}^1L_a$  and  ${}^1L_b$  states are significantly mixed, the internal conversion should be fast and only one lifetime should be observed on the nanosecond time scale.

The formation of an excited ICT state in methoxyanthracene also appears to be unlikely, because the electron-acceptor properties of the anthracene chromophore are rather poor. In particular, it has been shown already for a series of dialkoxy-substituted anthracene derivatives that only the 1,4-dialkoxyanthracene exhibits a significant excited-state ICT that is accompanied by a strong solvatochromism.<sup>21</sup> In contrast, no such ICT has been observed for the 2,3-dialkoxyanthracene. Similarly, the 2-methoxyanthracene does neither exhibit a charge-transfer absorption band, nor solvatochromic behavior. Moreover, the interconversion of the two emitting species, as indicated by the rise component in the emission lifetimes, is unlikely to be fast enough to compete with the emission rate; in particular since, at least in the ground state, the energy of activation for a *cis*–*trans* isomerization in olefins is usually so high that this reaction is prevented at standard conditions. Thus, we conclude that a charge-transfer excited state, that is accompanied by the formation of the isomeric intermediates *cis*-**1d**-ICT and *trans*-**1d**-ICT, is not responsible for the dual emission of 2-methoxy-substituted anthracene derivatives.

The observation of two lifetimes for the 2-methoxyanthracenes combined with the presence of a coupled process, along with the calculations performed and previous precedent in the literature are consistent with the assignment of the dual emission of 2-methoxyanthracenes to a torsional isomerization of the methoxy substituent. The growth kinetics of 2-methoxyanthracene derivatives, as well as the identical lifetimes detected at the emission maximum and at the emission wavelength of the long-lived component, indicate that the non-exponential decay is due to coupled processes. That is, the species with the short lifetime is transformed into the long-lived species leading to the growth in the emission intensity at the corresponding emission wavelength. If the two processes were uncoupled, i.e., two independent emitting species were present, decays with two lifetimes would have been observed at all wavelengths with no growth kinetics. It is important to note that the decay of the short-lived species can include other processes, such as intersystem crossing and internal conversion, besides the isomerization to the long-lived species. These results are—in the absence of other excited-state reactions such as proton transfer—characteristic of conformational changes in the excited state. Some anthracene derivatives with dual emission are already known, namely 2-vinylanthracene derivatives<sup>12b,c</sup> and *N*-methoxy-1-(2-anthryl)ethanimine.<sup>13</sup> In these cases, it has been shown that the two emissive species are conformational isomers, that are interconverted upon rotation about the C2–C<sub>vinyl</sub>– or C2–C<sub>imino</sub>–bond. Considering these observations, we propose that the 2-methoxyanthracene derivatives **1d**–**1g** also have two different preferential conformations in the ground and in the excited state, respectively, which are separated by a significant energy barrier. In fact, two independent calculations (CASSCF and DFT) reveal energy minima for two conformations of **1d**, namely, *s*-*cis* and *s*-*trans*, with the *s*-*cis* conformer being approximately 10 kJ/mol higher in energy in the ground state than the *s*-*trans* isomer. For the excited state, the CASSCF calculation gives the same trend, however, the difference of the energy is slightly higher (approximately 20 kJ/mol). Moreover, the difference between S<sub>0</sub> and S<sub>1</sub> was calculated to be slightly larger for the *s*-*cis* conformer than for the *s*-*trans* isomer. Therefore, excitation of the system leads to a nonequilibrium situation because it reflects the concentration ratios for both isomers in the ground state, whereas for the equilibrium in the excited-state the relative concentration of the *s*-*cis* conformer is lower. This change in the relative energies of the isomers is

responsible for the growth kinetics observed. Thus, the experimental and theoretical results give strong evidence for two emissive species resulting from two interconvertible ground- and excited-state conformers with significantly different energies. Considering the growth kinetics, when the fluorescence lifetime is recorded in the low-energy part of the overall emission spectrum, the origin of the short emission lifetime should be the transformation of the higher-energy conformation, i.e., the *s*-*cis* form, to the isomer that is lower in energy, i.e., the *s*-*trans* form. Thus, the latter conformer is assigned as the long-lived emissive species.

It should be noted, however, that although the calculations consistently support the proposal of the two conformers of **1d**, the electronic features of 2-methoxyanthracene are already too complex to be handled appropriately by either theoretical method employed. This can be seen from the unreasonably high energy barriers that are calculated for the conformational changes by the CASSCF method. From the experimental data, we estimated the barrier for rotation to be much lower and the estimated value of ca. 19 kJ/mol is in line with the experimentally obtained barriers for 2-vinylanthracene and *N*-methoxy-1-(2-anthryl)ethanimine derivatives (between 15–30 kJ/mol).<sup>12b,c,13</sup> Moreover, the rotational barrier of anisole was calculated to be approximately 12 kJ/mol.<sup>15</sup> Compared to the published data we employed higher-level calculations (CASSCF), however, at least in the case of methoxyanthracene this method overestimates the interaction of the free lone pairs of the oxygen atom with the  $\pi$  system of the anthracene. Nevertheless, the low-energy conformations *s*-*cis* and *s*-*trans* are in agreement with the ones calculated for 2-vinylanthracene<sup>12a</sup> and should, thus, reflect qualitatively the relative order of the ground- and excited-state energies.

The electron-donating properties of the methoxy substituent appear not to be an essential feature to provide the dual emission of the 2-methoxyanthracene derivatives, because a similar dual emission has been observed for *N*-methoxy-1-(2-anthryl)ethanimine.<sup>13</sup> In the latter compound, the rotating substituent is an electron-accepting group. Thus, the dual emission is established independent of the electron-donating and electron-accepting properties of the substituents; however, it cannot be excluded at the present stage that the interaction with the aromatic  $\pi$  system of anthracene, either donating or accepting, is a necessary requirement for dual emission of anthracene derivatives.

The fluorescence lifetimes of anthracene (**1a**), 2-methylanthracene (**1b**), and 2-chloroanthracene (**1c**), recorded in the present study with the same experimental setup used for the study of the 2-methoxyanthracenes, are in accordance with literature data<sup>22</sup> and the lifetimes determined by one of us previously;<sup>23</sup> i.e., a monoexponential decay with lifetimes between 3 and 5 ns was observed in each case. The comparison between anthracene derivatives **1b**, **1c**, and **1d** demonstrates that the substitution at the 2-position does not result in dual lifetimes in general, but that a methoxy substituent is required. This general trend is supported by the observation that all of the 2-methoxyanthracene derivatives tested in this study exhibit dual emission.

A literature report for some di(alkoxy)-substituted anthracene derivatives indicated that only single-exponential emission decays occurred, even for anthracenes with an alkoxy-substituent in the 2-position (2,3-di-(*n*-decyloxy)anthracene,  $\tau = 4.2$  ns; 2,6-di-(*n*-decyloxy)anthracene,  $\tau = 23.2$  ns).<sup>21</sup> In particular, it was pointed out in this report that the lifetimes of the latter compounds are essentially identical and the corresponding fits

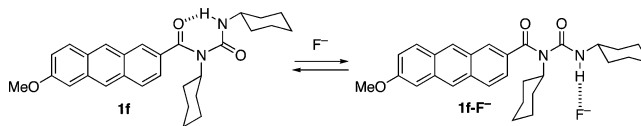
are the same, with either monoexponential or biexponential functions used for the deconvolution of the data. Thus, a monoexponential decay of the emission was assumed. Nevertheless, in a footnote it is mentioned that the loss of resolution in the fluorescence spectra of some derivatives is probably "due to the emission occurring from conformers which are kinetically indistinguishable with slightly different wavelength distributions."<sup>21</sup> Although we did not reinvestigate these compounds, we assume that it may be possible to resolve the dual emission as in the case of 2-methoxyanthracene **1d**, if the emission lifetime is detected at the high- and low-energy area of the emission band. It is also instructive to compare the lifetime of the *s*-cis isomer of **1d** with the ones obtained for other excited-state rotamers. Thus, the higher-energy conformers of 2-vinylanthracene and *N*-methoxy-1-(2-anthryl)ethanimine exhibit lifetimes of 3 and 6 ns at room temperature,<sup>12,13</sup> which is in good agreement with the short lifetimes of **1d** and **1e** (3–5 ns) and therefore provides further evidence that the rotational lifetimes are comparable in all of these systems.

The lifetimes detected for anthracene derivatives **1a–g** cover a remarkably broad range, i.e., from 4 to 27 ns. The intersystem crossing (ISC) in anthracenes occurs from the  $S_1$  state to  $T_2$ ,<sup>24</sup> and the  $S_1$ – $T_2$  state energy gap can be influenced with changes in the nature of the solvent or with the nature of substituents on the anthracene.<sup>25</sup> The long lifetimes observed for **1d–1h** compared to **1a** suggests that the  $S_1$ – $T_2$  energy gap is larger for the former compounds, decreasing the rate constant for ISC. In addition, the long lifetime for **1d** did not decrease when the temperature was raised suggesting that the  $T_2$  state was not accessible at 60 °C. The detailed mechanism for the substituent effect on the photophysics of anthracenes<sup>23</sup> is not clear since it seems to depend more on the position of the substituent than on its electronic nature. For this reason, the small changes in lifetimes for **1d–1h** in different solvents and in the presence and absence of analytes (**1f–1h**) cannot be interpreted at this point.

The original objective for this project was to extend the application of the fluorescent probes **1f–1h** toward lifetime-based sensing; i.e., different emission lifetimes were expected for the sensor in the absence and in the presence of the analyte. Nevertheless, the methoxy group, that was originally introduced to establish a push–pull pattern within the fluorophore, turned out to interfere with this approach as this structural feature alone already leads to two different emission lifetimes. Thus, the implementation of functionalities that give rise to the formation of conformers is counterproductive for the design of fluorescent probes and should be avoided whenever the emission lifetime is planned to be the indicating physical property. This drawback is especially pronounced in the case of the solvatochromic probe **1f**, however, the investigation of the emission lifetimes of pH-sensitive probes **1g** and **1h** revealed some additional information, regardless of the interfering dual lifetime due to the methoxy substituent.

The two pH-sensitive derivatives **1g** and **1h** exhibit the same dual fluorescence as the 2-methoxyanthracene. However, the change of the fluorescence lifetimes upon addition of acid is different for these two compounds. In the case of the anthryloxazoline **1g**, the emission lifetime of the longer-lived species decreases significantly from 13 to 9 ns upon addition of acid (pH 2), and the latter lifetime is assigned to the protonated form. Thus, in this case, the determination of the fluorescence lifetime represents a complementary method to the steady-state fluorimetric titrations. Nevertheless, it should be noted that the changes in the lifetimes are small and it would be hard to

## SCHEME 1



measure precisely the two lifetimes for conditions where protonated and unprotonated species were present. In contrast, the changes of the steady-state spectra are much more pronounced and the change of the emission color can be followed by the naked eye and may therefore be used on simple indicator plates without employing a spectrometer. Interestingly, the shorter lifetime remains the same within the error limit, suggesting that protonation had no effect on the decay of the *s*-cis isomer. Also, the lifetimes of both emitting transients of the pyridylanthracene **1h** do not change upon acidification, although significant changes are observed in the steady-state fluorescence. In the latter case it may be assumed that the lifetimes of **1h–H<sup>+</sup>** decreased to values that are below the detection limit of the equipment (1 ns), and the actually detected lifetimes are the ones of the remaining unprotonated form of **1h**.

In the case of the acylurea derivative **1f**, it was of particular interest whether the determination of the emission lifetimes in different solvents may help to elucidate the actual mechanism of the solvatochromic behavior of this compound. Such as in other solvatochromic systems, an internal charge transfer (ICT) due to a strong donor–acceptor interplay between the methoxyanthryl- and the *N*-acylureido functionalities in the excited-state is proposed.<sup>7</sup> The subsequent adiabatic ICT leads to an intermediate that most likely exhibits a region with development of negative charge that is, after solvent relaxation, stabilized by polar solvents, especially those with high acceptor number. This ICT–solvent relaxation sequence is consistent with the significant red shift of the emission spectra in polar solvents. In time-resolved experiments, such a behavior could potentially be supported by the corresponding TRES experiments in which the spectral relaxation may be followed. Unfortunately, the dual emission from the methoxyanthracene chromophore precludes experiments to detect the solvent relaxation with the time-resolved techniques employed in this study.

The addition of fluoride to the acylurea derivative **1f** results in a significant increase of the fluorescence lifetime of both the short- and long-lived transients, along with a hypsochromic shift of the emission maximum. It was previously shown that the cyclic hydrogen-bonded structure of the acylurea substituent has a pronounced influence on the emission properties of **1f**.<sup>7</sup> The change of the emission properties of **1f** upon fluoride addition originates from the cleavage of the intramolecular hydrogen bond between the amide NH and the carbonyl functionality in favor of the formation of a strongly bound amide–fluoride complex (Scheme 1). Thus, the change of the emission properties in the presence of fluoride is a secondary effect; i.e., it is not the direct result of the association of fluoride to the amide. Indeed, additional control experiments with the anthracene-carboxamide **1i** show that the formation of an amide–fluoride bond does not influence significantly the emission properties of the anthracene fluorophore. These results show that—in principle—the determination of the emission lifetime may be used complementary to the steady-state emission spectroscopy for the detection of fluoride ions with **1f**. It should be noted that although many fluoride sensors have been reported recently, it is certainly not the most relevant anion to be detected.<sup>26</sup> Nevertheless, it is demonstrated that the selective



destruction of the acylurea structure is a useful handle for fluorimetric detection either by steady-state or by lifetime-based methods and its structure may be varied such that other analytes trigger this modification of the substituent.

## Conclusion

We demonstrated that 2-methoxy-substituted anthracene derivatives exhibit a dual emission. Detailed investigations by time-resolved emission spectroscopy and additional theoretical studies support the proposal that the emissive transients originate from two interconvertible conformers, with *s*-cis and *s*-trans conformations relative to the exocyclic C2–O bond. This property interferes significantly with the establishment of lifetime-based sensing with donor–acceptor substituted anthracene derivatives. For this part it must be concluded that methoxy substituents, or rather alkoxy substituents in general, should be used with care in fluorescent probes that focus on time-resolved emission spectroscopy. On the other hand, it should be pointed out that the conformation-dependent dual fluorescence of 2-methoxyanthracene derivatives may find applications in other areas. Since the interconversion of the *s*-cis and *s*-trans conformers should very much depend on the surrounding environment, they may be used as lifetime-based probes to monitor the microenvironment, e.g., the available space in constrained or organized media.

**Acknowledgment.** H.I., A.G., and M.W. thank the Deutsche Forschungsgemeinschaft for generous financial support. C.B. and C.Y. thank the Natural Sciences and Engineering Council of Canada (NSERC) for funding. T.C.S.P. thanks NSERC for a Canadian Graduate Scholarship. We thank Prof. K.-H. Drexhage and Dr. J. Arden-Jacob, University of Siegen, for assistance with the HPLC analyses.

**Supporting Information Available:** Table S1, parameters for the fluorescence lifetime measurements of **1a–1i**; Figure S1, fluorescence decay of **1f** in acetonitrile in the presence and absence of fluoride; Figure S2, time-resolved emission spectra (TRES) of **1f** in acetonitrile in the presence of fluoride; Figure S3, fluorescence emission spectrum and emission lifetimes of **1i** in the absence and presence of fluoride; Figure S4, fluorescence decay of **1g** in the absence and in the presence of HCl; Figure S5, fluorescence decay of **1h** in the absence and in the presence of HCl; Figure S6, fluorescence excitation spectra for **1g** at 77 K; Table S2, lifetimes for **1d** at various temperatures; Figure S7, Arrhenius plot for the short lifetime of **1d**. This material is available free of charge via the Internet at <http://pubs.acs.org>.

## References and Notes

- (1) a) In *Optical Sensors*; Wolfbeis, O. S., Ed.; Springer-Verlag: Heidelberg, Germany, 2004. b) Mohr, G. J. *Chem. Eur. J.* **2004**, *10*, 1082–1090. c) Pu, L. *Chem. Rev.* **2004**, *104*, 1687. d) Martinez-Manez, R.; Sancenon, F. *Chem. Rev.* **2003**, *103*, 4419. e) Wiskur, S. L.; Ait-Haddou, H.; Anslyn, E. V.; Lavigne, J. J. *Acc. Chem. Res.* **2001**, *34*, 963. f) In *Chemosensors of Ion and Molecular Recognition*; Desvergne, J.-P., Czarnik, A. W., Eds.; Kluwer Academic Press: Dordrecht, The Netherlands, 1997. g) de Silva, A. P. H.; Gunaratne, Q.; Gunnlaugsson, T.; Huxley, A. J. M.; McCoy, C. P.; Rademacher, J. T.; Rice, T. E. *Chem. Rev.* **1997**, *97*, 1515. h) In *Fluorescent Chemosensors for Ion and Molecule Recognition*; ACS Symp. Ser. 538; Czarnik, A. W., Ed.; American Chemical Society: Washington D.C., 1993. (2) In *Topics in Fluorescence Spectroscopy, Probe Design and Chemical Sensing*; Lakowicz, J. R., Ed.; Plenum: New York, 1994; Vol. 4. (3) a) Lippitsch, M. E.; Draxler, S.; Kieslinger, D. *Sens. Act. B - Chem.* **1997**, *38*, 96–102. b) Szmazinski, H.; Lakowicz, J. R. *Sens. Act. B - Chem.* **1995**, *29*, 16–24. (4) a) Draxler, S.; Lippitsch, M. E. *Anal. Chem.* **1996**, *68*, 753–757. b) Lin, H.J.; Herman, P.; Kang, J. S.; Lakowicz, J. R. *Anal. Biochem.* **2001**, *294*, 118–125. (5) a) Anzenbacher, P., Jr.; Tyson, D. S.; Jursikova, K.; Castellano, F. N. *J. Am. Chem. Soc.* **2002**, *124*, 6232–6233. (6) Ihmels, H.; Meiswinkel, A.; Mohrschladt, C. J.; Otto, D.; Waidelich, M.; Towler, M.; White, R. *J. Org. Chem.* **2005**, *70*, 3929–3938. (7) Bohne, C.; Ihmels, H.; Waidelich, M.; Yihwa, C. *J. Am. Chem. Soc.* **2005**, *127*, 17158–17159. (8) **1d**: McCormick, F. A.; Marquart, D. J. *Tetrahedron Lett.* **1994**, *35*, 5169–5172.; **1e**: Ihmels, H. *Eur. J. Org. Chem.* **1999**, 1595–1600; **1f**: Ref. 7; **1g**: Ref. 6; **1h**: Ref. 6. (9) Ahlrichs, R.; Bär, M.; Baron, H.-P.; Bauernschmitt, R.; Böcker, S.; Furche, F.; Haase, F.; Häser, M.; Horn, H.; Hättig, C.; Huber, C.; Huniar, U.; Kattaneck, M.; Köhn, A.; Kölmel, C.; Kollwitz, M.; May, K.; Ochsenfeld, C.; Öhm, H.; Schäfer, A.; Schneider, U.; Sierka, M.; Treutler, O.; Unterreiner, B.; Arnim, M. V.; Weigend, F.; Weiss, P.; Weiss, H. *TURBOMOLE*, version 5; Universität Karlsruhe: Karlsruhe, Germany, 1998. (10) , Werner H.-J.; Knowles P. J.; Amos, R. D.; Bernhardtsson, A.; Bering, A.; Celani, P.; Cooper, D. L.; Degan, M. J. O.; Dobbyn, A. J.; Eckert, F.; Hampel, C.; Hetzer, G.; Knowles, P. J.; Korona, T.; Lindh, T.; Llyod, A. W.; McNicholas, S. J.; Manby, F. R.; Meyer, W.; Mura, M. E.; Nicklass, A.; Palmieri, P.; Pitzer, R. M.; Rauhut, G.; Schütz, M.; Schumann, U.; Stoll, H.; Stone, A. J.; Tarroni, R.; Thorsteinsson, T.; Werner, H.-J. *MOLPRO*, version 2002.1, University of Stuttgart, University of Cardiff, 2002. (11) Kawashima, Y.; Hashimoto, T.; Nakano, H.; Hirao, K. *Theor. Chem. Acc.* **1999**, *102*, 49–64. (12) a) Sakata, K.; Kometani, N.; Hara, K. *Chem. Phys. Lett.* **2001**, *344*, 185–192. b) Flom, S. R.; Nagajan, V.; Barbara, P. F. *J. Phys. Chem.* **1986**, *90*, 2085–2092. c) Brearley, A. M.; Flom, S. R.; Nagajan, V.; Barbara, P. F. *J. Phys. Chem.* **1986**, *90*, 2092–2099. (13) Furuuchi, H.; Arai, T.; Sakuragi, H.; Tokumaru, K.; Nishimura, Y.; Yamazaki, I. *J. Phys. Chem.* **1991**, *95*, 10322–10325. (14) McWeeny, R. *Methods of Molecular Quantum Mechanics*, 2nd ed.; Academic Press: London, 1978. (15) Tsuzuki, S.; Houjou, H.; Nagawa, Y.; Hiratani, K. *J. Phys. Chem. A* **2000**, *104*, 1332–1336. (16) Fulde, P. *Electron Correlations in Molecules and Solids*; Springer Series in Solid State Sciences; Springer, Berlin, 1995; Vol. 100. (17) Birks, J. B. *Photophysics of Aromatic Molecules*; Wiley-Interscience: London, 1970. (18) Wolf, J.; Hohlneicher, G. *Chem. Phys.* **1994**, *181*, 185–208. (19) (a) Kleevens, H. B.; Platt, J. R. *J. Chem. Phys.* **1949**, *17*, 470–481. (b) Bergman, A.; Jortner, J. *Chem. Phys. Lett.* **1972**, *15*, 309. (c) Steiner, R. P.; Michl, J. *J. Am. Chem. Soc.* **1978**, *100*, 6861–6867. (d) Lambert, W. R.; Felker, P. M.; Syage, J. A.; Zewail, A. H. *J. Chem. Phys.* **1984**, *81*, 2195–2208. (20) Friedrich, D. M.; Mathies, R.; Albrecht, A. C. *J. Mol. Spectros.* **1974**, *51*, 166–188. (21) Brotin, T.; Desvergne, J.-P.; Fages, F.; Utermöhlen, R.; Bonneau, R.; Bouas-Laurent, H. *Photochem. Photobiol.* **1992**, *55*, 349–358. (22) **1a**: a) Lampert, R. A.; Chewter, L. A.; Phillips, D.; O'Connor, D. V.; Roberts, A. J.; Meech, S. R. *Anal. Chem.* **1983**, *55*, 68–73. b) Blatt, E.; Treloar, F. E.; Ghiggino, K. P.; Gilbert, R. G. *J. Chem. Phys.* **1981**, *85*, 2810–2816. **1b**: c) Weber, G.; Shinitzky, M.; Dianoux, A. C.; Gitler, C. *Biochemistry* **1971**, *10*, 2106–2113. d) Vembe, T. M.; Kiyanskay, L. A.; Cherkaso, A. S. *Zh. Obs. Khim.* **1963**, *33*, 2342. e) **1c**: Bright, F. V.; McGown, L. B. *Anal. Chem.* **1985**, *57*, 55–59. (23) Bohne, C.; Kennedy, S. R.; Boch, R.; Negri, F.; Orlandi, G.; Siebrand, W.; Scaiano, J. C. *J. Phys. Chem.* **1991**, *95*, 10300–10306. (24) a) Ware, W. R.; Baldwin, B. A. *J. Chem. Phys.* **1965**, *43*, 1194. b) Bennett, R. G.; McCartin, P. J. *J. Chem. Phys.* **1966**, *44*, 1969. c) Lim, E.C.; Lapos, J. D.; Yu, J. M. H. *J. Mol. Spectrosc.* **1966**, *19*, 412. d) Kellogg, R. E. *J. Chem. Phys.* **1966**, *43*, 411. (25) Hamanoue, K.; Hidaka, T.; Nakayama, T.; Teranishi, H.; Sumitani, M.; Yoshihara, K. *Bull. Chem. Soc. Jpn.* **1983**, *56*, 1851. (26) Martinez-Manez, R.; Sancenon, F. *Chem. Rev.* **2003**, *103*, 4419.